ARTICLE

Notoginsenoside R1 protects against myocardial ischemia/reperfusion injury in mice via suppressing TAK1-JNK/p38 signaling

Jing-jing Zeng[1,2,3], Han-qing Shi[1], Fang-fang Ren[1], Xiao-shan Zhao[1], Qiao-ying Chen[1], Dong-juan Wang[2], Lian-pin Wu[1], Mao-ping Chu[1], Teng-fang Lai[4✉] and Lei Li[1✉]

Previous studies show that notoginsenoside R1 (NG-R1), a novel saponin isolated from *Panax notoginseng*, protects kidney, intestine, lung, brain and heart from ischemia-reperfusion injury. In this study we investigated the cardioprotective mechanisms of NG-R1 in myocardial ischemia/reperfusion (MI/R) injury in vivo and in vitro. MI/R injury was induced in mice by occluding the left anterior descending coronary artery for 30 min followed by 4 h reperfusion. The mice were treated with NG-R1 (25 mg/kg, *i.p.*) every 2 h for 3 times starting 30 min prior to ischemic surgery. We showed that NG-R1 administration significantly decreased the myocardial infarction area, alleviated myocardial cell damage and improved cardiac function in MI/R mice. In murine neonatal cardiomyocytes (CMs) subjected to hypoxia/reoxygenation (H/R) in vitro, pretreatment with NG-R1 (25 μM) significantly inhibited apoptosis. We revealed that NG-R1 suppressed the phosphorylation of transforming growth factor β-activated protein kinase 1 (TAK1), JNK and p38 in vivo and in vitro. Pretreatment with JNK agonist anisomycin or p38 agonist P79350 partially abolished the protective effects of NG-R1 in vivo and in vitro. Knockdown of TAK1 greatly ameliorated H/R-induced apoptosis of CMs, and NG-R1 pretreatment did not provide further protection in TAK1-silenced CMs under H/R injury. Overexpression of TAK1 abolished the anti-apoptotic effect of NG-R1 and diminished the inhibition of NG-R1 on JNK/p38 signaling in MI/R mice as well as in H/R-treated CMs. Collectively, NG-R1 alleviates MI/R injury by suppressing the activity of TAK1, subsequently inhibiting JNK/p38 signaling and attenuating cardiomyocyte apoptosis.

Keywords: myocardial ischemia/reperfusion injury; notoginsenoside R1; TAK1; JNK; p38; apoptosis

Acta Pharmacologica Sinica (2023) 44:1366–1379; https://doi.org/10.1038/s41401-023-01057-y

INTRODUCTION

Coronary artery disease (CAD) is one of the leading causes of morbidity and mortality worldwide [1]. Reperfusion (including thrombolysis, coronary bypass surgery, and percutaneous coronary intervention) is a standard treatment for CAD and has been used widely, but the incidence of heart damage remains high [2, 3]. One of the reasons is myocardial ischemia/reperfusion (MI/R) injury, which can lead to severe arrhythmia, myocardial dysfunction, robust inflammatory responses and myocardial necrosis or apoptosis [4–7]. Therefore, novel medications and therapeutics to reduce MI/R injury that are complementary to current reperfusion therapies are urgently needed.

Extensive cell necrosis or apoptosis and an excessive inflammatory response are two aspects of MI/R pathology [8–11]. Therefore, interrupting the positive feedback loop can effectively ameliorate heart damage. Several molecular events are activated during MI/R injury, such as mitogen-activated protein kinase (MAPK) signaling, which participates in apoptotic and inflammatory responses through the activation and/or inactivation of the three critical subfamilies p38 mitogen-activated protein kinase (p38 MAPK), c-Jun N-terminal kinase (JNK), and extracellular signal-regulated kinase (ERK) [12–14]. Previous studies have demonstrated that activation of JNK/p38 signaling exacerbates M/IR injury [5]. Inhibiting the activation of p38 and JNK (SB239063 and SP600125, respectively) improved myocardial and mitochondrial abnormalities in rats with MI/R injury [15]. Transforming factor β-activated kinase 1 (TAK1) belongs to the mitogen-activated kinase kinase (MAPKKK) family and is involved in a variety of biological responses, including inflammation, apoptosis, and survival in different cell types [16–18]. Once activated, TAK1 activates the MAPK kinases MKK4 and MKK3/6, which phosphorylate p38 MAPK and JNK, respectively. Studies have shown that the activation of TAK1 in mice can further activate NF-κB, p38 MAPK and JNK, thus increasing inflammation and inducing apoptosis or even death [19–22]. Previous studies have demonstrated that Dusp14 prevents hepatic I/R injury by inhibiting TAK1 [23]. Our previous study demonstrated that TAK1 was activated in mice after MI/R, and TAK1 silencing ameliorated MI/R-induced

Notoginsenoside R1 protects against myocardial ischemia/reperfusion injury
JJ Zeng et al.

1367

myocardial dysfunction and myocardial injury [24]. Therefore, effective intervention of these critical regulators could aid in the development of novel clinical treatments for MI/R injury.

Panax notoginseng is a traditional Chinese herb that has been used to treat cardiovascular and cerebrovascular diseases for a long time in China [25, 26]. Notoginsenoside R1 (NG-R1), a major component isolated from *Panax notoginseng*, is the main bioactive compound in many traditional Chinese medicines, such as Xuesaitong, Naodesheng, XueShuanTong, ShenMai, and QSYQ. Therefore, this compound has significant potency in drug development [27]. NG-R1 is a novel phytoestrogen that exerts many cardioprotective effects through the suppression of oxidative stress, inflammation and apoptosis [25, 28, 29]. For example, NG-R1 ameliorated brain damage in an oxygen-glucose deprivation/reoxygenation (OGD/R) rat model by activating the estrogen receptor to downregulate the JNK signaling pathway [30]. In addition, it inhibited inflammation and apoptosis, decreased p38 MAPK and increased the expression of Bcl-2 in rat renal ischemia-reperfusion injury [31]. NG-R1 deactivated the TGFβ1/TAK1 signaling pathway and protected the heart against lung ischemia-reperfusion injury in rabbits [32]. Previous studies indicated that NG-R1 exerted pharmacological effects on ischemia-reperfusion injury in the kidney, intestine, lung, brain and heart [27, 29, 32, 33]. However, the detailed mechanism of NG-R1 in MI/R injury in mice remains unclear.

In the present study, we used gene overexpression and silencing to investigate the molecular mechanism underlying the cardioprotective effects of NG-R1 on MI/R injury and obtained insights into the cardioprotective mechanisms.

MATERIALS AND METHODS

Materials
NG-R1 was purchased from Sigma (St. Louis, MO, USA). The molecular structure of NG-R1 is shown in Fig. 1b. Evans blue and 2,3,5-triphenyltetrazolium chloride (TTC) were purchased from Sigma (St. Louis, MO, USA). ELISA kits for cardiac troponin I (cTnI) and creatine kinase-MB (CK-MB) were purchased from Shanghai Westang Bio-tech Co., Ltd. (Shanghai, China). Anisomycin and P79350 were purchased from Calbiochem (La Jolla, CA, USA). Small interfering RNAs (siRNAs) against TAK1 were obtained from Guangzhou RiboBio (Guangzhou, China). Recombinant adeno-associated virus serotype 9 (AAV9) vectors harboring TAK1 or GFP with a c-TnT promoter (AAV9-cTnT-GFP, AAV9-cTnT-TAK1) were obtained from Taitool Bioscience (Shanghai, China).

Animals and MI/R injury in vivo
The animal use and care protocol conformed to the Guide for the Care and Use of Laboratory Animals from the National Institutes of Health and was approved by the Animal Care and Use Committee of Wenzhou Medical University (Number: wydw2017-0081). Male C57/BL6 mice (age, 7–8 weeks; weight, 20–25 g) were purchased from the SLAC Laboratory Animal Centre of Shanghai (Shanghai, China). The animals (4/cage) were acclimated for two weeks before the experiment and could freely consume standard mouse chow and water in a temperature-controlled room with a 12 h light-dark cycle. The MI/R injury model was established by occluding the left anterior descending coronary artery (LAD) as described previously [24]. In short, the anesthetized mice were intubated and ventilated with isoflurane (1.5% v/w) at a respiratory rate of 140–160 and tidal volume of 250–300 μl/min (Ventilator-Hugo Sachs Elektronic MiniVent Type 845, Germany). Then, a transverse incision was made along the upper edge of the third or fourth rib, and the heart was exposed. When the entire LAD was exposed, the distal 1/3 of the LAD was ligated with 7–0 silk sutures. After coronary artery occlusion for 30 min, the slipknot was released for 4 h (to examine protein expression and myocardial infarct size) and 24 h (to analyze cardiac function).

Sham-operated mice were anesthetized, and the suture was placed under the LAD but without ligation.

Animal groupings and treatments
The phase 1 experimental design is shown in Fig. 1a. Male C57/BL6 mice were randomly allocated to four groups: (1) In the sham group, mice underwent the sham operation and were injected i.p. with normal saline (the solvent for NG-R1). (2) In the NG-R1 group, mice underwent the sham operation and were injected i.p. with 25 mg·kg^{-1} NG-R1 for a total of three injections. (3) In the MI/R group, mice were subjected to the MI/R operation and were injected i.p. with normal saline. (4) In the MI/R + NG-R1 group, the mice were treated with NG-R1 30 min prior to ischemic surgery and then subjected to MI/R, as previously described [29]. In the phase 2 study, recombinant adeno-associated virus serotype 9 (AAV9) vectors harboring TAK1 or GFP with a c-TnT promoter (AAV9-cTnT-GFP, AAV9-cTnT-TAK1) were used to examine the effects of NG-R1 on the myocardium in TAK1-overexpressing mice challenged by MI/R [24]. The experimental design is shown in Fig. 8a. The mice were randomly allocated to four groups: (1) In the MI/R + AAV9-cTnT-GFP group, the mice were injected through the tail vein with AAV9-cTnT-GFP vectors (3 × 10^{11} vector genomes/mouse) 5 weeks prior to the operation and were then subjected to MI/R. (2) In the MI/R + AAV9-cTnT-GFP + NG-R1 group, the mice were treated with AAV9-cTnT-GFP vectors 5 weeks prior to operation and then subjected to MI/R with NG-R1 (25 mg·kg^{-1}). (3) In the MI/R + AAV9-cTnT-TAK1 group, the mice were treated with AAV9-cTNT-TAK1 vectors 5 weeks prior to the operation and were then subjected to MI/R. (4) In the MI/R + AAV9-cTnT-TAK1 + NG-R1 group, the mice were treated with AAV9-cTnT-TAK1 vectors 5 weeks prior to the operation and were then subjected to MI/R with NG-R1.

Evans blue/TTC double-staining
Evans blue/TTC double-staining was performed to evaluate the infarct size as previously described [24]. Briefly, the LAD was reoccluded 4 h after reperfusion, and 2% Evans blue dye was perfused via the inferior vena cava. Then, the heart was removed, sliced and incubated with 1% TTC (Sigma–Aldrich, St Louis, Mo) for 20 min at 37 ℃. The myocardial infarct size (INF), area at risk (AAR), and left ventricular (LV) size of each slice were analyzed by Image-Pro Plus software.

TUNEL staining
Heart tissues were embedded in OCT for sectioning (5 μm). Terminal deoxynucleotidyl transferase dUTP nick end labeling (TUNEL, Roche Diagnostics) was used to examine myocardial apoptosis according to the manufacturer's instructions. Images were collected with a Nikon ECLIPSE Ti microscope (Olympus BX51, Tokyo, Japan).

Biochemical analyses
The cTnI and CK-MB concentrations in mouse plasma were quantified using commercial ELISA kits (Shanghai Westang Bio-tech Co., Ltd., China) according to the manufacturer's instructions.

Echocardiographic and hemodynamic analysis
Transthoracic echocardiography was preformed as previously described [19, 24]. Briefly, the mice were ventilated with isoflurane (1.5% v/w), and then an echocardiography system (15-MHz linear transducer, Vevo1100, Visual Sonics, Canada) was used to assess cardiac function 14 days after reperfusion. M-mode images were recorded from the long axis of the left ventricle at the papillary muscle level, and then the left ventricular ejection fraction (LVEF) and left ventricular short-ening (LVFS) were measured.

Masson's trichrome staining
To assess fibrosis 14 days after MI/R, the heart tissues were washed with PBS, fixed with 4% paraformaldehyde solution overnight,

paraffin-embedded and sectioned into 5 μm sections. The sections were then stained with Masson's trichrome and observed under a microscope (Leica Microsystems GmbH).

Hypoxia/reoxygenation (H/R) model
Murine neonatal cardiomyocytes (CMs) were isolated from 1- to 3-day-old neonatal C57/BL6 mouse hearts as described previously [24]. Subsequently, the cardiomyocytes were seeded into 6-well plates at a density of 2×10^6 cells per well. After 24 h, the CMs were treated with glucose-free DMEM (Gibco, 11966-25, USA) in a tri-gas incubator with 95% N_2 and 5% CO_2 for 6 h, followed by 6 h of normal culture conditions to induce reoxygenation injury as described previously [24].

Cell treatments
Cells were pretreated with the JNK agonist anisomycin (25 ng/mL) or the p38 agonist P79350 (50 mmol/L) for 1 h prior to NG-R1 administration. TAK1 siRNA (Guangzhou RiboBio, China) and the negative control siRNA were mixed with Lipofectamine 2000 (Cat# 11668027, Thermo Fisher Scientific, USA) for transfection according to the manufacturer's instructions. The CMs were harvested 48 h after transfection and used for further analysis. The CMs were plated in 6-well plates and transfected with TAK1 overexpression adenoviral vectors and control GFP vectors (GeneChem Co., Ltd., Shanghai, China) at an MOI of 20 as previously described [24]. Briefly, adenoviral vectors were added to the cells and incubated for 24 h. After the medium was replaced, the cells were cultured for another 24 h. The CMs were treated with or without NG-R1 (25 μM) for 24 h prior to H/R treatment.

MTS cell viability assay and lactate dehydrogenase activity assay
The number of viable CMs was evaluated by the CellTiter 96 ® Aqueous One Solution Cell Proliferation Assay MTS kit (Cat# G3582, Promega, Madison, WI, USA). Briefly, 20% MTS dye solution was added to each well and incubated for 2.5 h, and the absorbance at 480 nm was recorded. Lactate dehydrogenase (LDH) activity was measured using a standard assay (Cat# G7891, Promega, Madison, WI, USA) according to the manufacturer's directions. The MTS assay and LDH assay were repeated three times to maintain consistency.

Determination of the apoptosis ratio by flow cytometry
The CMs were examined with a FITC Annexin V apoptosis detection kit (cat# 556547, BD Biosciences, Franklin Lakes, NJ, USA) or a PE Annexin V apoptosis detection kit (cat# 559763, BD Biosciences, USA) according to the manufacturer's protocols. Apoptosis was detected by flow cytometry (Cytomic FC 500MCL, Beckman), and the apoptosis ratio was quantified by BD FACS software. The experiments were repeated three times.

Real-time PCR analysis
Total RNA was isolated from CMs using TRIzol reagent (Invitrogen, USA) and reverse transcribed into cDNA using TransScript One-Step gDNA Removal and cDNA Synthesis SuperMix (Transgen Biotech, China). The expression levels of α-SMA, Collagen I, and Fibronectin were detected by real-time PCR using IQ SYBR Green Supermix (Bio-Rad, USA). β-actin was used as the internal reference. The following primers were used for analysis:
β-actin forward primer: 5′-TGAGCTGCGTTTTACACCCT-3′
β-actin reverse primer: 5′-TTTGGGGGATGTTTGCTCCA-3′
α-SMA forward primer: 5′-CCTTCGTGACTACTGCCGAG-3′
α-SMA reverse primer: 5′-ATAGGTGGTTTCGTGGATGC-3′
Collagen I forward primer: 5′-TTCTCCTGGCAAAGACGGAC-3′
Collagen I reverse primer: 5′-CTCAAGGTCACGGTCACGAA-3′
Fibronectin forward primer: 5′-CCCCAACTGGTTACCCTTCC-3′
Fibronectin reverse primer: 5′-TGTCCGCCTAAAGCCATGTT-3′

Western blot analysis
Treated cells or the border zones of the infarcted hearts were homogenized in RIPA lysis buffer (cat# 89900, Thermo Fisher, USA) containing protease inhibitors (Beyotime, Jiangsu, China, ST506-2) and a protease inhibitor cocktail (cat# 4906837001, Roche, Switzerland). The protein concentration was determined by a BCA Protein Assay Kit (Beyotime, Shanghai, China). Equal amounts of protein (50 μg) were separated on SDS polyacrylamide gels (10%–15%) and transferred to polyvinylidene difluoride (PVDF) membranes (Thermo Fisher, Waltham, MA, USA). The membranes were then blocked for 2 h at room temperature in 5% milk. Subsequently, the membranes were incubated with relevant primary antibodies overnight at 4 °C, followed by incubation with the appropriate HRP-conjugated secondary antibodies (mouse or rabbit antibody, 1:10000, Cell Signaling Technology). The proteins were quantified by Image-Pro Plus (Bio-Rad) and normalized against β-actin. The antibodies used were anti-JNK (cat# 9252, CST, Danvers, MA, USA), anti-p-JNK (Thr183/Tyr185) (81E11) (cat# 4668, CST, Danvers, MA, USA), anti-ERK (137F5) (cat# 4695, CST, Danvers, MA, USA), anti-p-ERK (Thr202/Tyr204) (D13.14.4E) (cat# 4370, CST, Danvers, MA, USA), anti-p-p38 (Thr180/Tyr182) (D3F9) (cat# 4511, CST, Danvers, MA, USA), anti-p38 (D13E1) (cat# 8690, CST, Danvers, MA, USA), anti-TAK1 (cat# ab109526, Abcam, Cambridge, MA, USA), anti-p-TAK1 (CST, Danvers, MA, USA), anti-Bcl-2 (cat# ab59348, Abcam, Cambridge, MA, USA), anti-Bax (cat# 2772, CST, Danvers, MA, USA), and anti-β-actin (13E5) (cat# 4970, CST, Danvers, MA, USA).

Statistical analysis
Data were analyzed using SPSS 20.0 (IBM Analytics, Chicago, IL, USA) and are expressed as the mean ± SEM. Statistical analyses were performed using a two-tailed unpaired Student's t test for two-group comparisons. Multiple comparisons were evaluated by one-way analysis of variance (ANOVA) followed by Dunnett's multiple comparison test where appropriate. $P < 0.05$ was considered significant.

RESULTS
NG-R1 attenuates MI/R injury-induced myocardial damage and apoptosis
To further clarify the effect of NG-R1 on MI/R injury, NG-R1 was intraperitoneally injected total of three times into the mice 30 min before ischemia (Fig. 1a) [29]. Plasms levels of cTn-I and CK-MB were increased after MI/R injury (Fig. 1c, d). However, these increases were inhibited by NG-R1 treatment, with reductions in cTn-I levels to 4.733 ± 0.09 ng/ml and CK-MB levels to 184.0 ± 3.15 U/L (both $P < 0.01$ compared to the MI/R group) in plasma. The myocardial infarct size was measured by Evans blue dye-TTC double staining 4 h after reperfusion (Fig. 1e). The white area represents the infarcted area, the red area represents the ischemic myocardium, and the blue area represents the non-ischemic myocardium. No infarct area was observed in the sham group or NG-R1 group. The AAR/LV ratio was not different between the MI/R group and MI/R + NG-R1 group (Fig. 1f), indicating consistency in the MI/R model. However, compared with that in the MI/R group, the INF/AAR ratio was lower in the MI/R + NG-R1 group (67.67% ± 1.83% *vs.* 36.50% ± 2.06%, $P < 0.01$, Fig. 1f). Myocardial apoptosis is an important characteristic of MI/R-induced injury. As shown in Fig. 1h, a large number of TUNEL-positive cells as observed in the peri-infarct zone after MI/R injury, whereas treatment with NG-R1 markedly reduced the number of TUNEL-positive cells (Fig. 1g, h). In addition, Western blotting was performed to analyze cardiac Bcl-2 and Bax protein expression in the border zone (Fig. 1i). The expression of Bax was increased after MI/R injury and was decreased by NG-R1 (Fig. 1j). Similarly, NG-R1 treatment blocked the downregulation of Bcl-2 expression after MI/R injury (Fig. 1j).
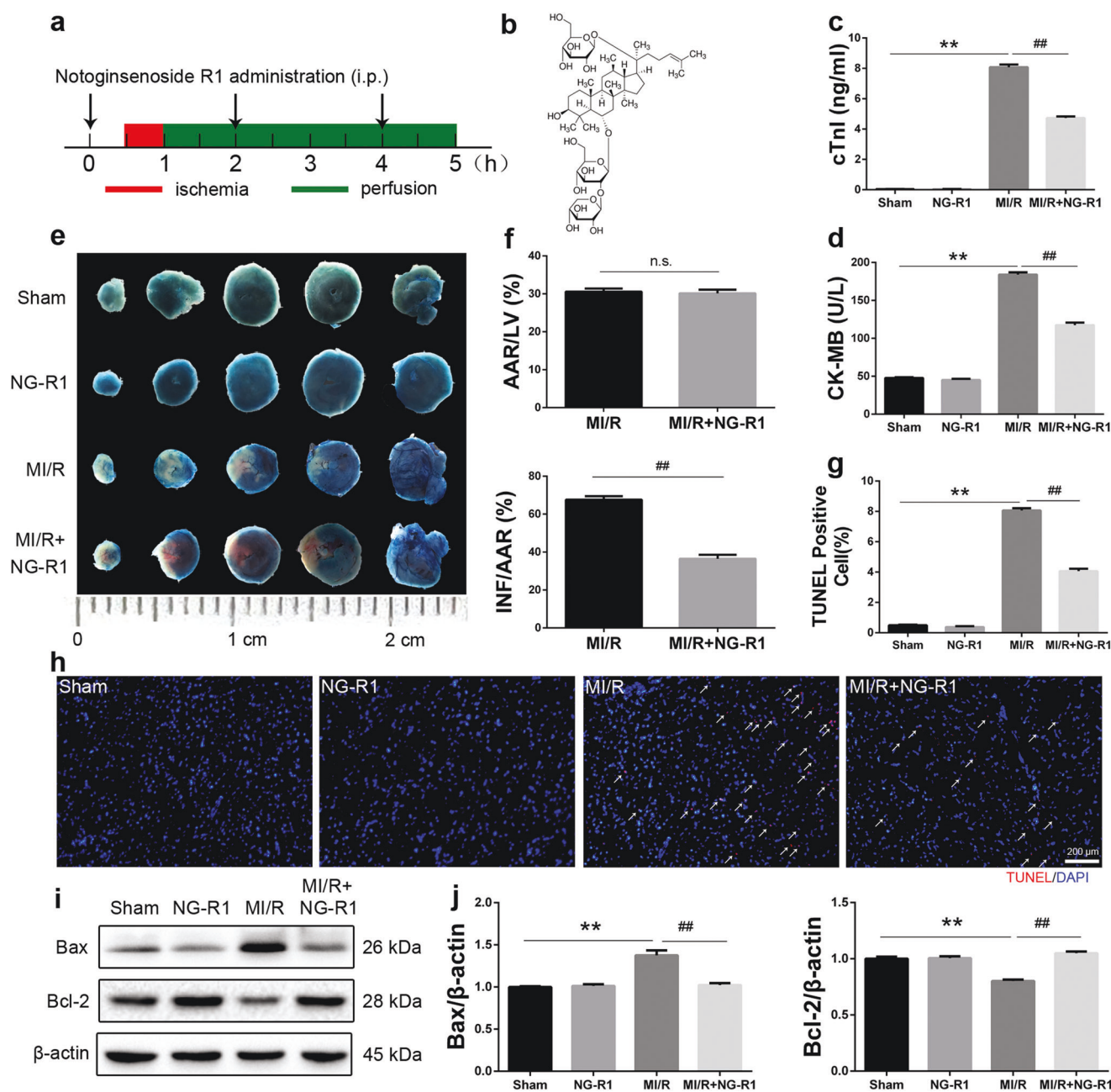
Notoginsenoside R1 protects against myocardial ischemia/reperfusion injury
JJ Zeng et al.

1369

Fig. 1 NG-R1 ameliorates MI/R injury in vivo. a Schematic illustration of the NG-R1 treatment protocol. NG-R1 (25 mg·kg^{-1} dissolved in normal saline) was intraperitoneally injected into C57/BL6 mice a total of three times. The mice were divided into the sham group (Sham), NG-R1 group (NG-R1), MI/R group (MI/R), and MI/R + NG-R1 group (MI/R + NG-R1). Normal saline was administered in the sham group. **b** Molecular structure of NG-R1. **c** Cardiac troponin-I (cTnI) levels in plasma 4 h after perfusion. **d** Cardiac creatine kinase-MB (CK-MB) levels in plasma 4 h after perfusion. **e** Representative infarct images obtained by Evans blue/TTC staining in each group. The infarct size (INF: white area), the area at risk (AAR: red and white area), and the nonischemic area (blue). Scale bar = 1 cm. **f** The ratio of the area at risk to the left ventricle and the ratio of the infarct size to the area at risk based on. **g, h** Representative immunofluorescence images showing TUNEL (red) staining in the infarct border zone. Scale bar = 200 µm. **i, j** Protein expression levels of Bax and Bcl-2 were analyzed by Western blotting. β-actin served as a loading control. The data are shown as the mean ± SEM (n = 6 for each group). **P < 0.01 *vs.* the Sham group. ##P < 0.01 *vs.* the MI/R group.

NG-R1 ameliorates MI/R-induced cardiac dysfunction and fibrosis To evaluate the protective effect of NG-R1, noninvasive echocardiography was used to assess cardiac function 14 days after reperfusion (Fig. 2a, b). MI/R injury induced left ventricular dysfunction, as shown by decreases in the LVEF and LVFS compared to those in the Sham group, while treatment with NG-R1 improved the LVEF (36.50% ± 1.25% *vs.* 50.67% ± 2.60%,

P < 0.01) and LVFS (17.83% ± 1.01% *vs.* 24.33% ± 1.49%, P < 0.05). Masson's trichrome staining showed that the collagen deposition area of myocardial fibrosis was increased in response to MI/R injury. NG-R1 decreased cardiac fibrosis during MI/R (Fig. 2c, d). In addition, an attenuated fibrotic effect was observed in the MI/R + NG-R1 group, as indicated by the reduced mRNA expression of α-SMA, Collagen I, and fibronectin (Fig. 2e).
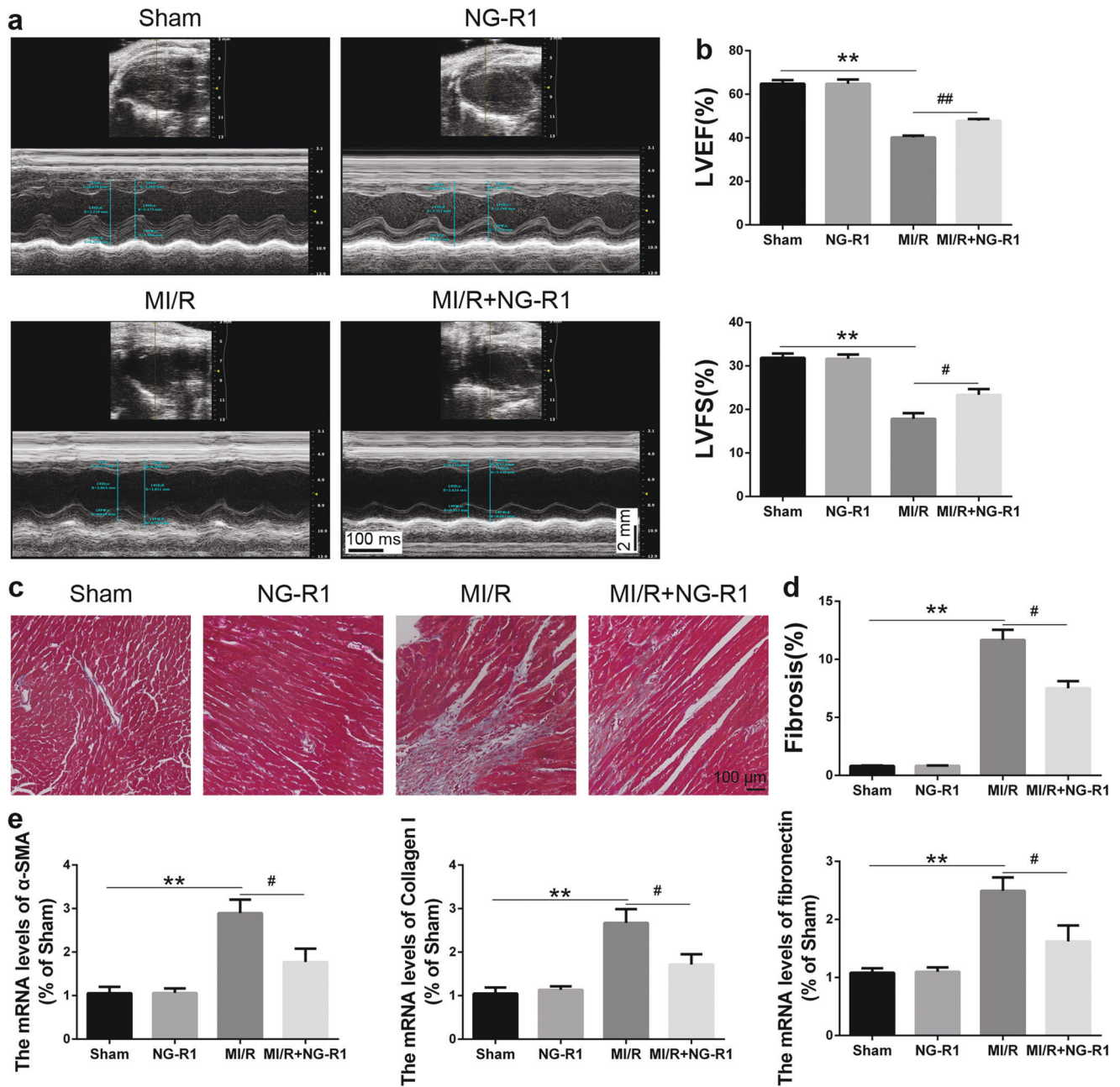
Notoginsenoside R1 protects against myocardial ischemia/reperfusion injury
JJ Zeng et al.

1370

Fig. 2 NG-R1 prevents MI/R injury-induced cardiac remodeling and dysfunction. a Representative images of M-mode echocardiography in each group. **b** Quantitative echocardiographic analysis of left ventricular ejection fraction (LVEF) and left ventricular fractional shortening (LVFS). **c, d** Representative images of Masson trichrome-stained MI/R hearts and quantification of the fibrosis area (%). Scale bar = 100 μm. **e** Quantitative reverse transcription polymerase chain reaction analysis of α-SMA, collagen I and fibronectin. The data are represented as the mean ± SEM (n = 6 for each group). **P < 0.01 vs. the Sham group. #P < 0.05 and ##P < 0.01 vs. the MI/R group.

NG-R1 protects murine neonatal cardiomyocytes from H/R-induced cell death

To further examine the antiapoptotic effect of NG-R1 on MI/R injury, murine neonatal cardiomyocytes (CMs) were subjected to 6 h of hypoxia and then reoxygenated for 6 h (Fig. 3a). Dose–response experiments showed that the optimal concentration of NG-R1 in CMs was 25 μM (Fig. 3b, c). NG-R1 treatment restored the viability of CMs after H/R injury, as demonstrated by MTS assays, LDH release assays and visual inspection (Fig. 3b-d). In parallel, the proportion of TUNEL-positive cells in the H/R group was much higher than that in the Control group, while the proportion in the H/R + NG-R1 group was markedly lower than that in the H/R group (Fig. 3e, f). In addition, flow cytometry indicated that H/R

injury increased the proportion of apoptotic cells, and this effect was reduced by NG-R1 pretreatment (Fig. 3g, h). Moreover, NG-R1 pretreatment decreased the expression of Bax and increased the expression of Bcl-2 in CMs after H/R injury (Fig. 3i, j).

Protective effects of NG-R1 involve JNK/p38 signaling

The results suggested that NG-R1 ameliorated the cardiac injury induced by MI/R in vivo and in vitro. Next, we conducted experiments to examine which signaling pathway was responsible for cardiomyocyte apoptosis during MI/R. The MAPK signaling pathway plays an important role in cardiomyocyte apoptosis during MI/R [34]. To clarify whether the MAPK pathway participated in apoptosis during MI/R, the phosphorylation of
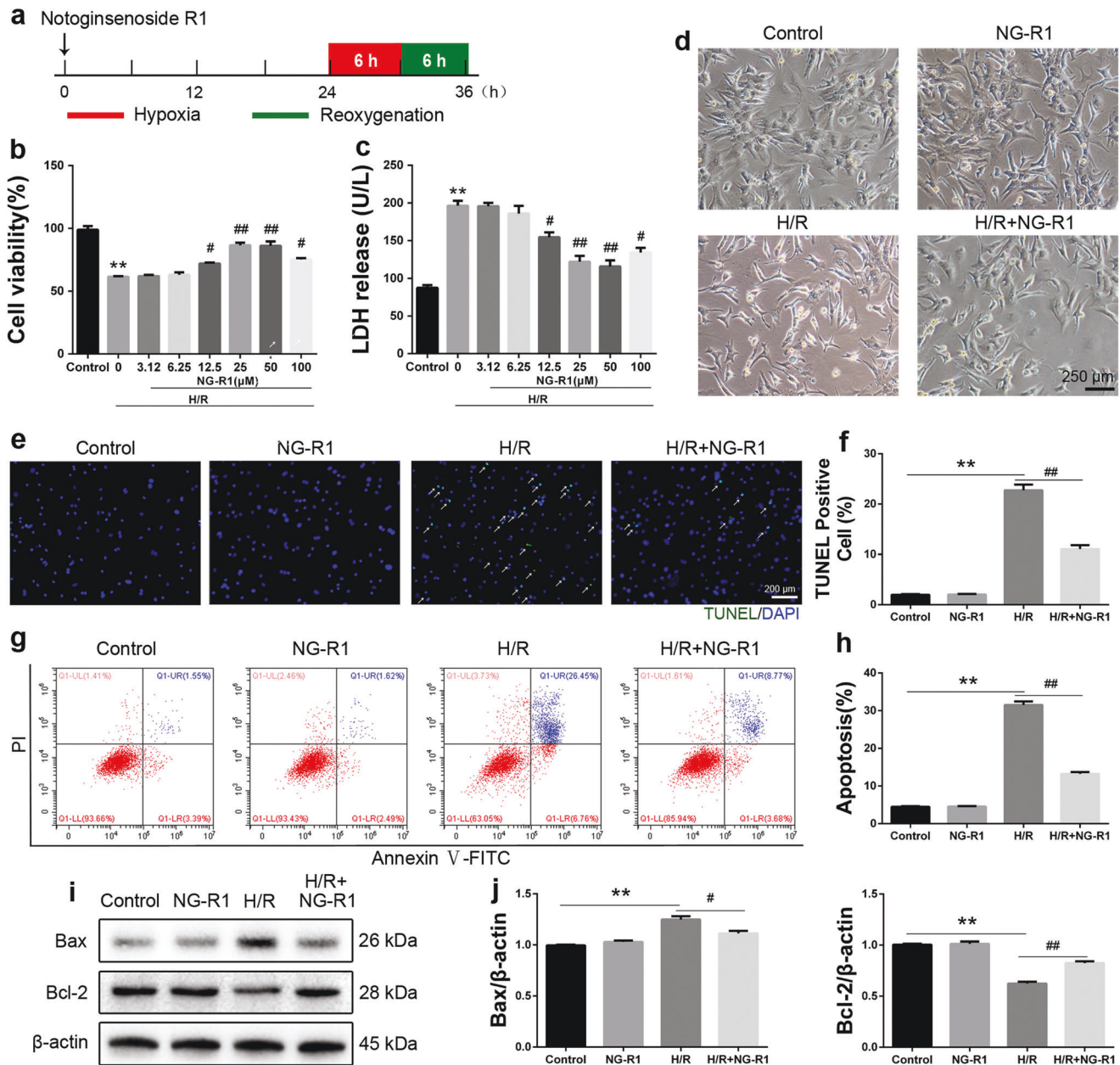
Notoginsenoside R1 protects against myocardial ischemia/reperfusion injury
JJ Zeng et al.

1371

Fig. 3 NG-R1 treatment attenuates neonatal cardiomyocytes (CMs) death in mice subjected to H/R. a Schematic illustration of H/R injury in CMs. **b** The viability of CMs after NG-R1 pretreatment (0, 3.12, 6.25, 12.5, 25, 50, 100 μM) for 24 h was analyzed by MTS assays. **c** Cell damage was determined by an LDH release assay. **d** Representative morphology of CMs in the control group (control), NG-R1 group (NG-R1), H/R group (H/R) and H/R + NG-R1 group (H/R + NG-R1). Scale bar = 250 μm. **e** Immunofluorescence staining of TUNEL-positive cells. Scale bar = 200 μm. **f** Quantitative analysis of (**e**). **g, h** Representative images showing apoptosis were determined by FITC-PI/Annexin V staining. The apoptosis rate of each group was determined. **i, j** The expression levels of Bcl-2 and Bax were measured by Western blotting. β-actin served as a loading control. The data are shown as the mean ± SEM ($n = 6$ for each group). **P < 0.01 vs. the Control group. #P < 0.05 and ##P < 0.01 vs. the H/R group.

p38 (p-p38), JNK (p-JNK) and ERK (p-ERK) was measured by Western blotting. MI/R surgery activated MAPK signaling (Fig. 4a, b), which was indicated by the increased levels of p-p38, p-JNK and p-ERK after MI/R injury. However, NG-R1 treatment abolished the activation of p38 and JNK but not ERK. Consistent with this finding, H/R injury activated p38, JNK and ERK, as determined by Western blot analysis, and the administration of NG-R1 attenuated the activation of p38 and JNK but not ERK (Fig. 4c, d).

To further identify the effect of NG-R1 on the deactivation of JNK/p38 signaling, anisomycin (a JNK agonist) and P79350 (a p38 agonist) were used. After pretreatment with anisomycin or P79350,

the reduction in the proportion of TUNEL-positive H/R + NG-R1-treated CMs (Fig. 7f, g) was abrogated, and the decrease in the proportion of total apoptotic cells was partially nullified (Fig. 4g, h), blocking the protective effects of NG-R1 against apoptosis. Furthermore, the mice were intraperitoneally injected with anisomycin or tail vein-injected with P79350 to confirm the effects of JNK/p38 signaling. The results showed that the reduction in the proportion of TUNEL-positive cells (Fig. 5a, b), the improvements in the echocardiography parameters (Fig. 5c, d), the decrease in cardiac fibrosis (Fig. 5e, f), and the downregulation of fibrosis marker mRNA expression (Fig. 5g) in the MI/R + NG-R1 group were
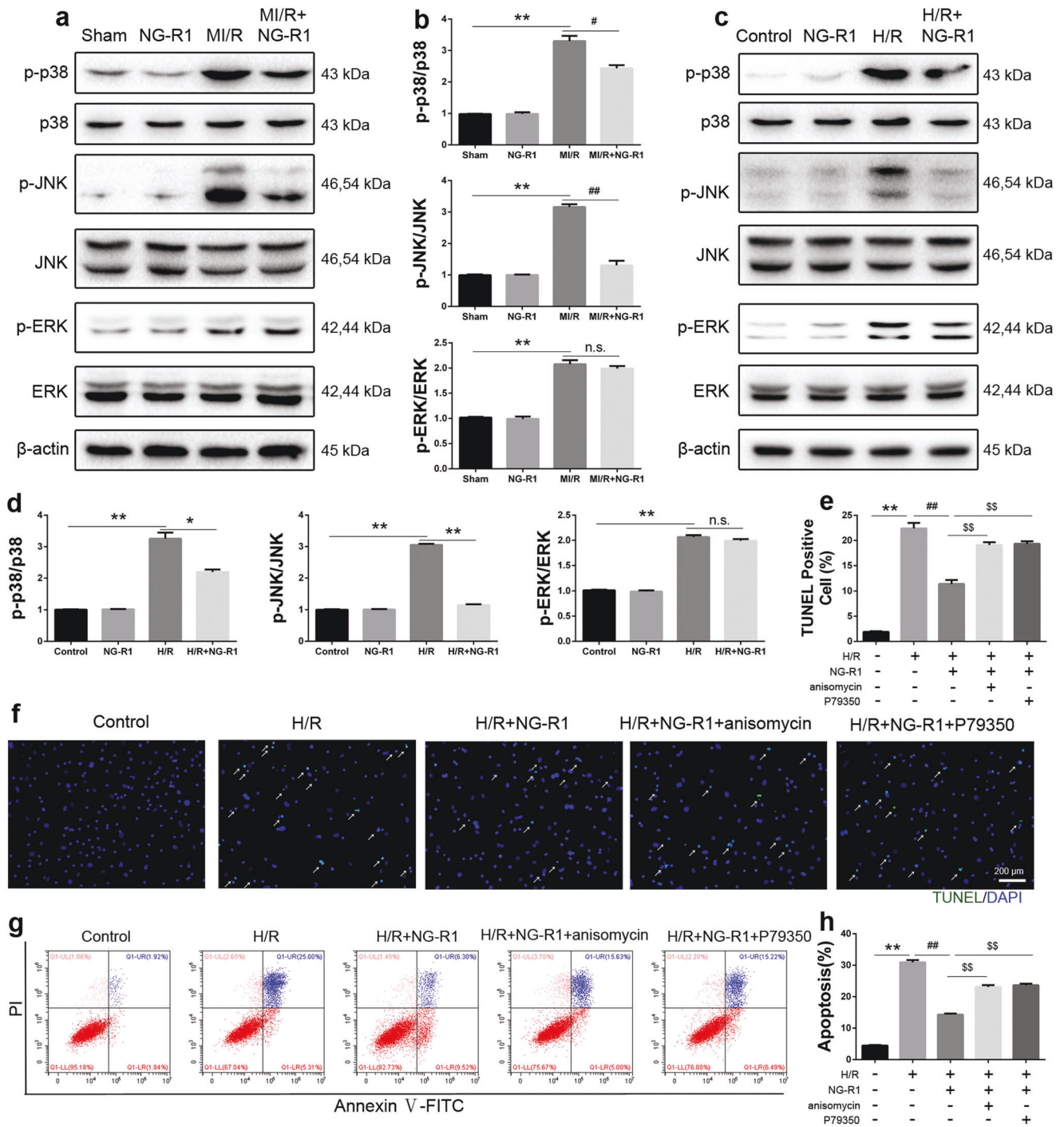
Notoginsenoside R1 protects against myocardial ischemia/reperfusion injury
JJ Zeng et al.

1372

Fig. 4 NG-R1 inhibits activation of the JNK/p38 signaling pathway after MI/R. a Western blot analysis of phosphorylated and total p38, JNK and ERK protein levels in ischemic myocardial tissue 4 h after perfusion. β-actin served as a loading control. **b** Quantitative analysis of **a**. **c** Western blot analysis of phosphorylated and total p38, JNK and ERK protein levels in vitro. **d** Quantitative analysis of **c**. **e, f** Representative images and quantitative analysis of TUNEL-positive cells. Scale bar = 200 μm. **g** Representative images of apoptosis were determined by FITC-PI/Annexin V staining. **h** Statistical analysis of apoptosis in the five groups. The data are shown as the mean ± SEM ($n = 6$ for each group). $*P < 0.05$ and $**P < 0.01$ *vs.* the Sham group or the Control group. $\#P < 0.05$ and $\#\#P < 0.01$ *vs.* the MI/R group or the H/R group. $^{\$\$}P < 0.01$ *vs.* the H/R + NG-R1 group.

abolished by anisomycin or P79350. These results demonstrated that the protective effects of NG-R1 involve JNK/p38 signaling.

TAK1 is the target of the protective effect of NG-R1 against MI/R injury
TAK1 plays a critical role in the regulation of cardiomyocyte death and MI/R injury [35–38]. Our previous study showed that

inhibiting TAK1 ameliorated MI/R injury [24]. To elucidate the detailed mechanism of NG-R1 in MI/R injury, the phosphorylation of TAK1 (p-TAK1) was measured. The level of p-TAK1 was upregulated after MI/R injury, and NG-R1 treatment inhibited the activation of TAK1 (Fig. 6a, b). Consistent with this finding, H/R-induced activation of TAK1 was also inhibited in the H/R + NG-R1 group (Fig. 6c, d). In addition, CMs were infected with an
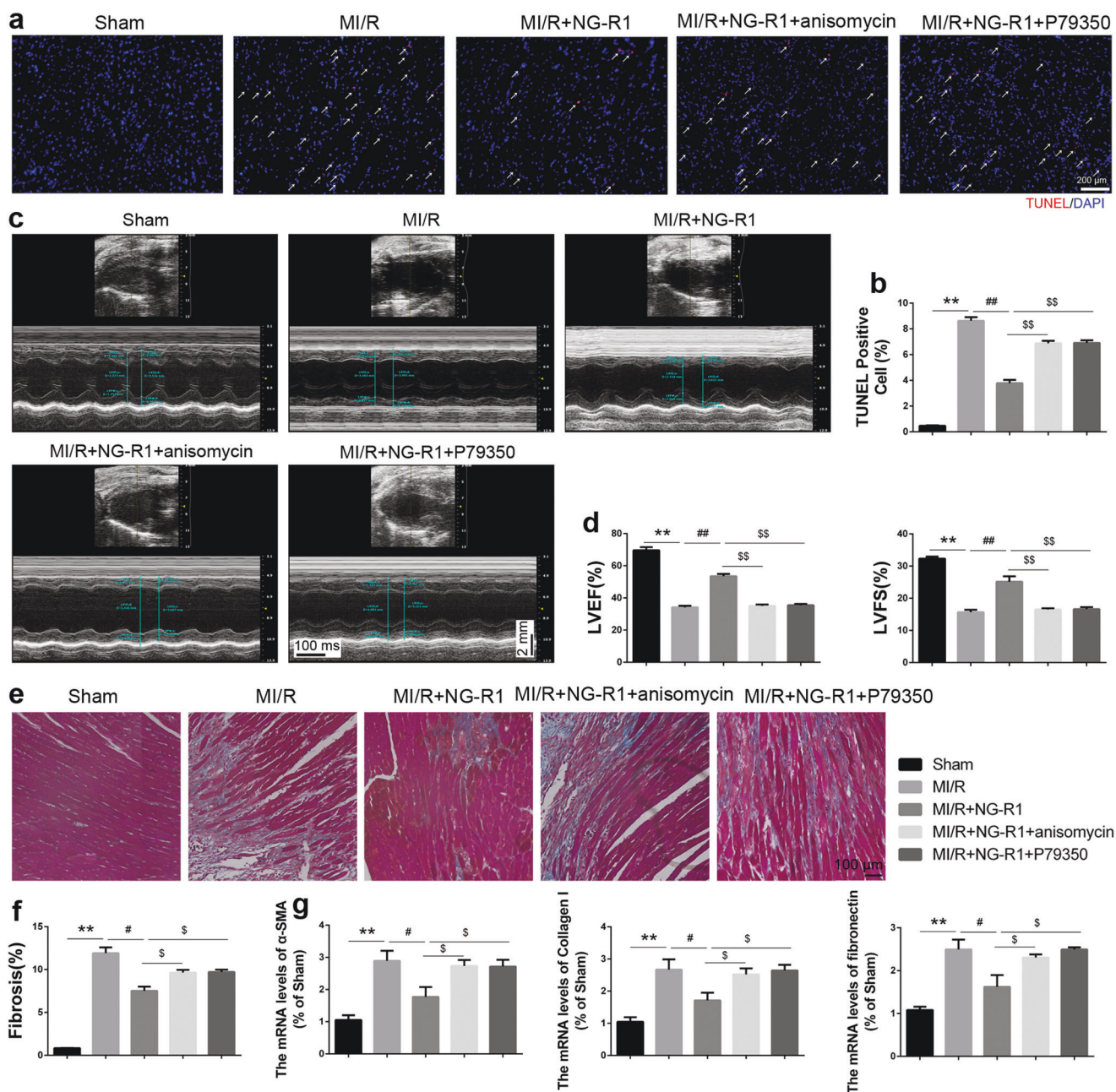
Notoginsenoside R1 protects against myocardial ischemia/reperfusion injury
JJ Zeng et al.

1373

Fig. 5 The protective effects of NG-R1 involve JNK/p38 signaling. a Representative immunofluorescence images showing TUNEL (red) staining in the infarct border zone in the various groups. Scale bar = 200 μm. **b** Quantitative analysis of **a**. **c** Representative images of M-mode echocardiography in each group. **d** Quantitative echocardiographic analysis of LVEF and LVFS. **e, f** Representative images of Masson trichrome-stained MI/R hearts and quantification of the fibrosis area (%). Scale bar = 100 μm. **g** Quantitative reverse transcription polymerase chain reaction analysis of α-SMA, collagen I and fibronectin. The data are represented as the mean ± SEM (n = 6 for each group). **P < 0.01 vs. the Sham group. #P < 0.05 and ##P < 0·01 vs. the MI/R group. $P < 0.05 and $$P < 0.01 vs. the MI/R + NG-R1 group.

adenoviral vector expressing TAK1 to verify whether TAK1 mediates the effects of NG-R1 on H/R injury (Fig. 6e). Compared with that in the H/R + Ad-GFP group, administration of NG-R1 decreased the proportion of TUNEL-positive cells (Fig. 6f, g), reduced the proportion of total apoptotic cells (Fig. 6h, i), decreased the expression of Bax and increased the expression of Bcl-2 in CMs (Fig. 6j, k). These effects were abrogated in the H/R + NG-R1 group that was pretreated with Ad-TAK1. Taken together, these results suggested that TAK1 overexpression abolished the protective effect of NG-R1 on H/R-induced cardiomyocyte apoptosis. After pretreatment with Ad-TAK1, the protein levels of p-TAK1, p-p38 and p-JNK in the H/R + Ad-

TAK1 + NG-R1 group were higher than those in the H/R + NG-R1 group (Fig. 6j, k). This finding suggests that NG-R1 plays an antiapoptotic role via TAK1-JNK/p38 signaling in vitro.

To further determine whether TAK1 was indispensable for the protective effect of NG-R1 against H/R injury, si-TAK1 was used (Fig. 7a). Compared with that in the H/R + si-NC group, TAK1 silencing reduced the proportion of TUNEL-positive cells (Fig. 7b, c), decreased the proportion of apoptotic cells (Fig. 7d, e), suppressed the activity of TAK1, p38 and JNK, decreased the expression of Bax and increased the expression of Bcl-2 in CMs (Fig. 7f, g). Intriguingly, NG-R1 plus si-TAK1 did not provide further protection against H/R-induced cardiomyocyte apoptosis (Fig. 7b-g).
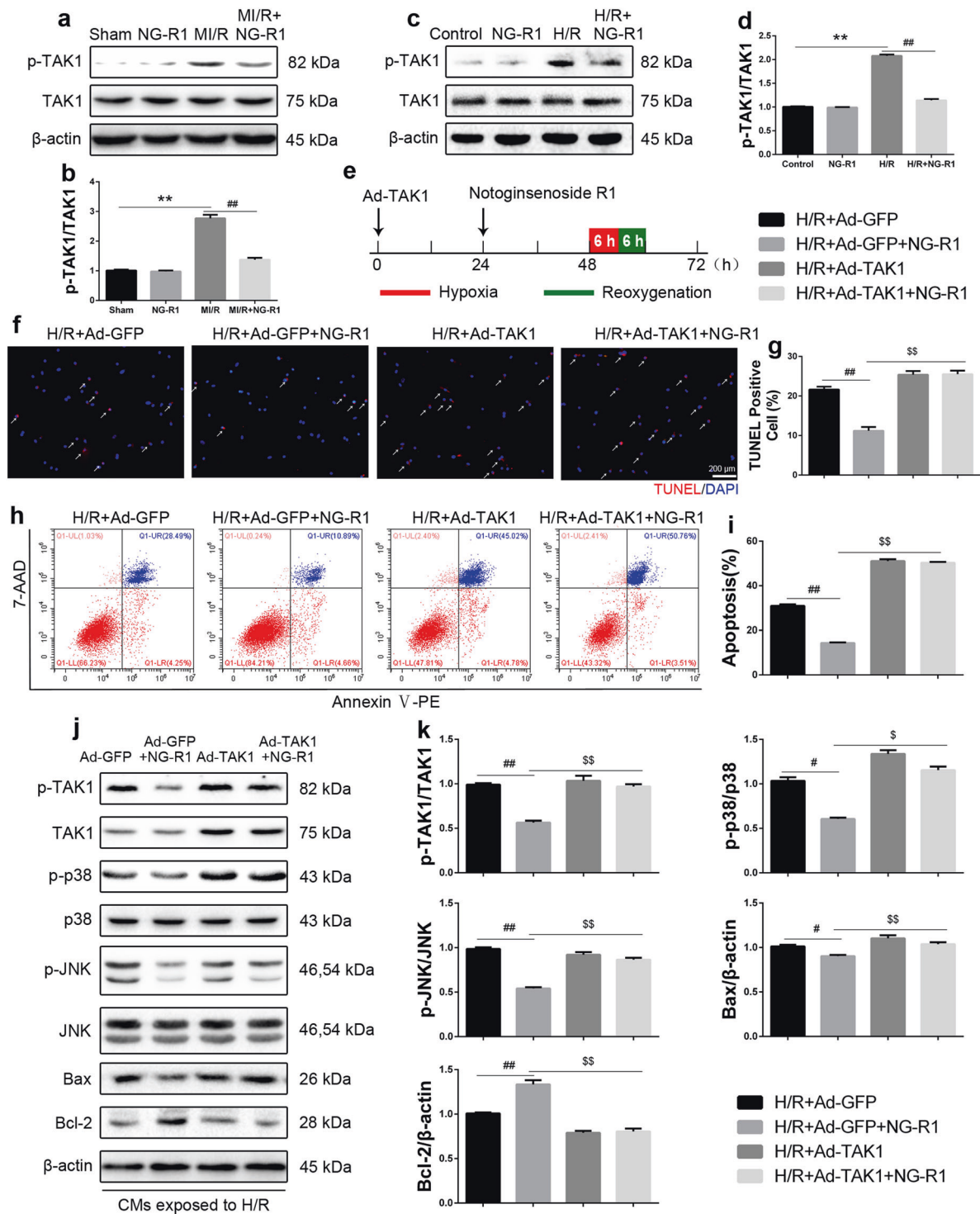
Notoginsenoside R1 protects against myocardial ischemia/reperfusion injury
JJ Zeng et al.

1374

Fig. 6 TAK1 overexpression reversed the antiapoptotic effect of NG-R1 on CMs. a Western blot analysis of phosphorylated and total TAK1 protein levels in ischemic myocardial tissue 4 h after perfusion. β-actin served as a loading control. **b** Quantitative analysis of **a**. **c** Western blot analysis of phosphorylated and total TAK1 protein levels in vitro. **d** Quantitative analysis of **c**. **e** Schematic illustration of TAK1 adenoviral infection. The TAK1 overexpression adenoviral vector or control GFP adenovirus (20 MOI) was used to infect CMs 48 h before H/R injury. **f** Immunofluorescence staining of TUNEL-positive cells. Scale bar = 200 μm. **g** Quantitative analysis of **f**. **h** Representative images of apoptosis, as determined by PE-7-AAD/Annexin V staining. **I** Statistical analysis of apoptosis in the four groups. **j** The expression levels of p-TAK1, TAK1, p-p38, p38, p-JNK, JNK, Bcl-2 and Bax were determined by Western blotting. **k** Quantitative analysis of **j**. The data are shown as the mean ± SEM ($n = 6$ for each group). **$P < 0.01$ *vs*. the Sham group or the Control group. #$P < 0.05$ and ##$P < 0.01$ *vs*. the MI/R group, the H/R group or the H/R + Ad-GFP group. $$P < 0.05$ and $$$P < 0.01$ *vs*. The H/R + Ad-GFP + NG-R1 group.

Notoginsenoside R1 protects against myocardial ischemia/reperfusion injury
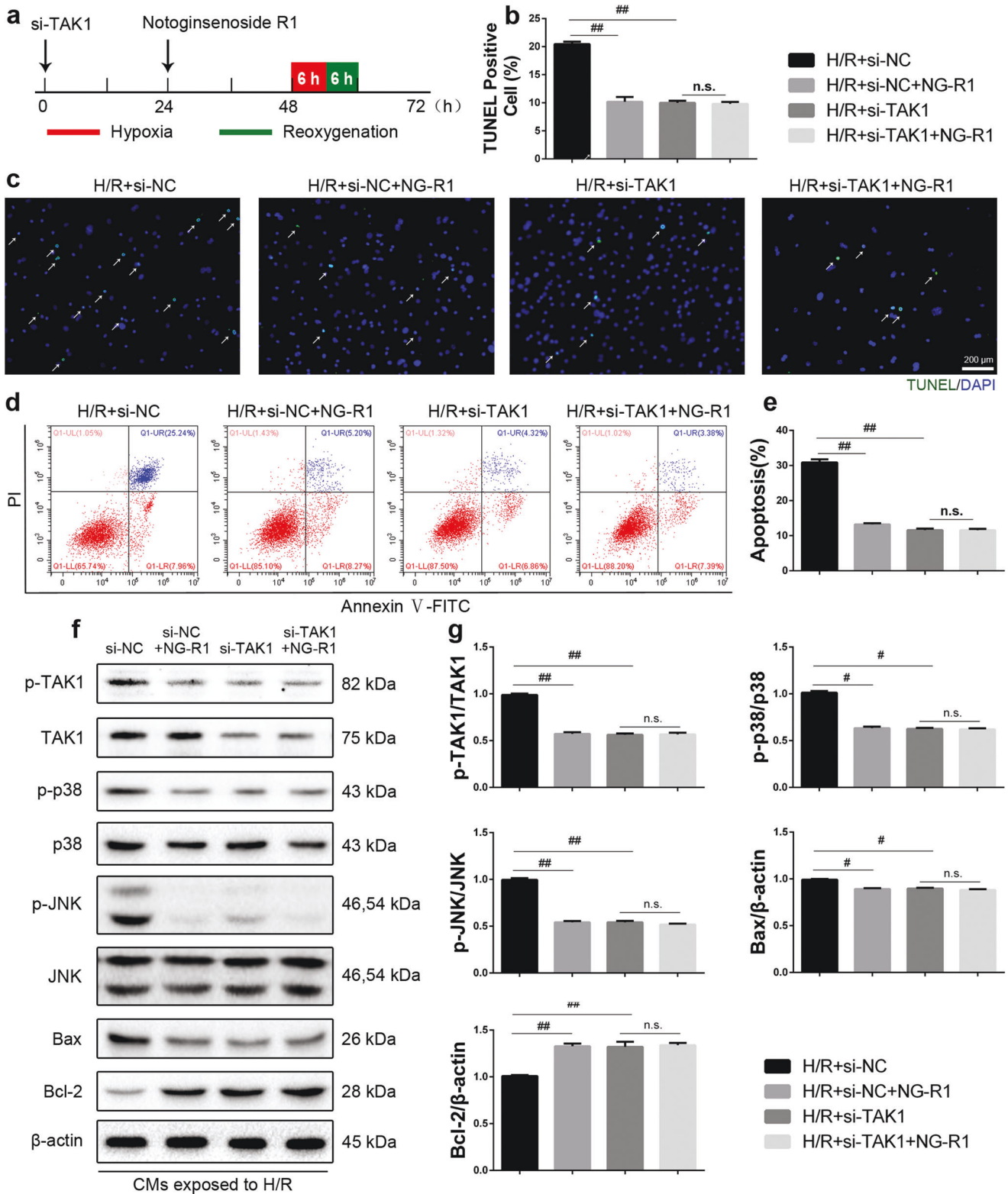JJ Zeng et al.

1375

Fig. 7 NG-R1 inhibits H/R-induced apoptosis in CMs by suppressing TAK1. a Schematic illustration of si-TAK1 transfection. CMs were transfected with si-TAK1 48 h before H/R injury. **b**, **c** Representative images and quantitative analysis of TUNEL-positive cells. Scale bar = 200 μm. **d** Representative images of apoptosis, as determined by FITC-PI/Annexin V staining. **e** Statistical analysis of apoptosis in the four groups. **f** The protein levels of p-TAK1, TAK1, p-p38, p38, p-JNK, JNK, Bcl-2 and Bax were determined by Western blotting. **g** Quantitative analysis of **f**. The data are shown as the mean ± SEM ($n = 6$ for each group). #$P < 0.05$ and ##$P < 0.01$ vs. the H/R + si-NC group.

Notoginsenoside R1 protects against myocardial ischemia/reperfusion injury
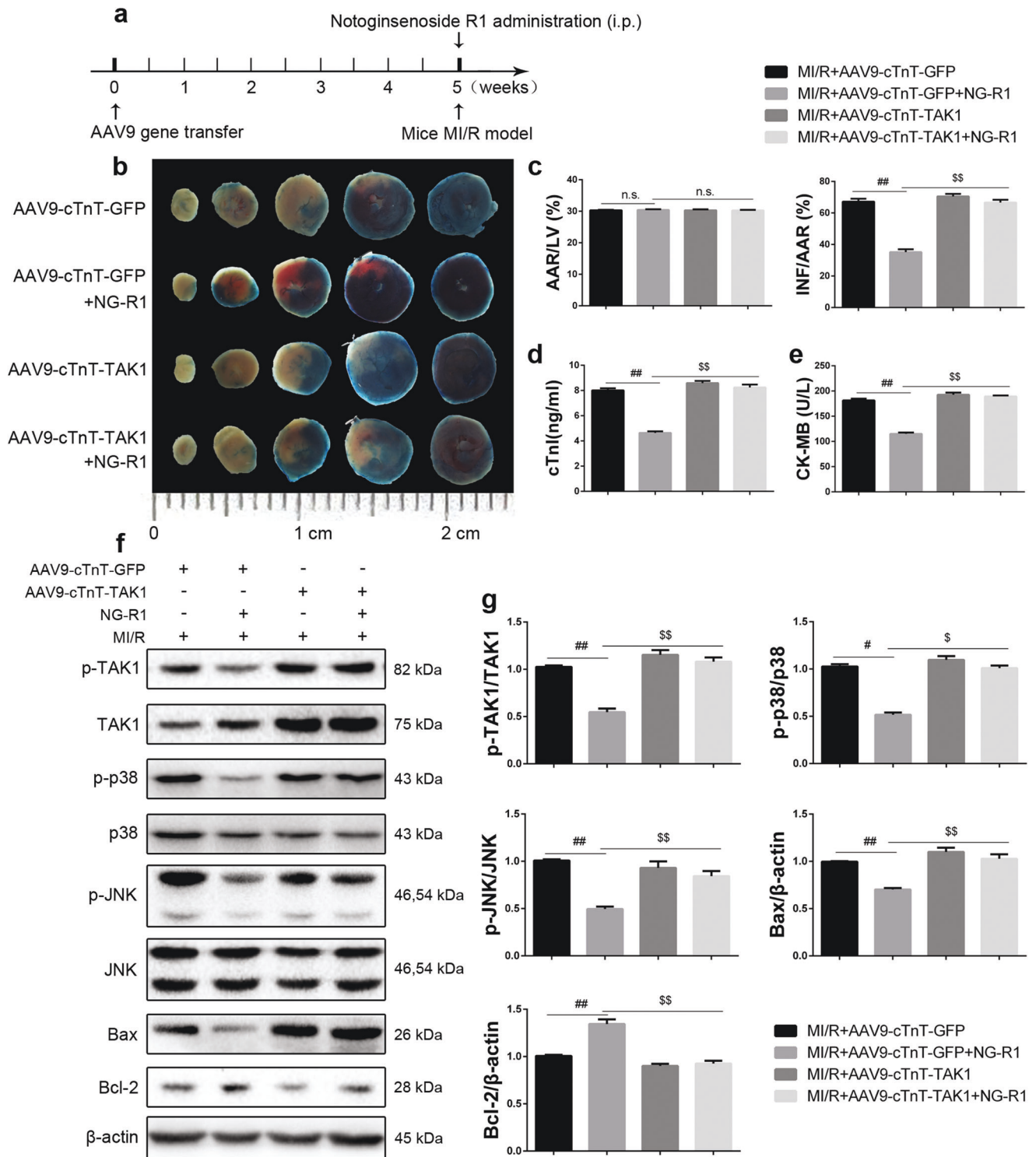JJ Zeng et al.

1376

Fig. 8 TAK1 overexpression reversed the protective effect of NG-R1 on MI/R injury. a The time course of AAV9-mediated TAK1 overexpression. Recombinant AAV9 vectors harboring TAK1 or GFP with a c-TnT promoter [3×10^{11} vector genomes/mouse] were injected into the tail veins of the mice 5 weeks before MI/R. **b, c** Representative infarct images obtained by Evans blue/TTC staining in each group. **d** Cardiac troponin-I (cTnI) levels in plasma 4 h after perfusion. **e** Cardiac creatine kinase-MB (CK-MB) levels in plasma 4 h after perfusion. **f, g** Western blot images and quantitative analysis of p-TAK1, TAK1, p-p38, p38, p-JNK, JNK, Bcl-2 and Bax protein expression in ischemic myocardial tissue. The data are shown as the mean ± SEM ($n = 6$ for each group). $^{#}P < 0.05$ and $^{##}P < 0.01$ *vs.* the MI/R + AAV-cTnT-GFP group. $^{$}P < 0.05$ and $^{$$}P < 0.01$ *vs.* the MI/R + AAV9-cTnT-GFP + NG-R1 group.

To further confirm the role of TAK1 in mediating the effects of NG-R1 on MI/R injury, we used an AAV9 vector with a cTnT promoter to selectively overexpress TAK1 in vivo [24]. TAK1-overexpressing mice were then subjected to MI/R and administered NG-R1 (Fig. 8a). The improvements in the INF/AAR ratio and the plasma levels of cTnI and CK-MB in the MI/R + AAV9-cTnT-GFP + NG-R1 group were abolished by TAK1 overexpression (Fig. 8b-e). In addition, compared with those in the MI/R + AAV9-

Notoginsenoside R1 protects against myocardial ischemia/reperfusion injury
JJ Zeng et al.

1377

cTnT-GFP + NG-R1 group, the protein level of Bax was increased and the protein level of Bcl-2 was decreased in the MI/R + AAV9-cTnT-TAK1 + NG-R1 group (Fig. 8f, g). TAK1 overexpression markedly increased the activity of TAK1, p38 and JNK in the MI/R + AAV9-cTnT-TAK1 + NG-R1 group (Fig. 8f, g). Furthermore, the decrease in TAK1-JNK/p38 signaling was restored in the MI/R + AAV9-cTnT-TAK1 + NG-R1 group (Fig. 8f, g). These results demonstrated that TAK1-JNK/p38 signaling may be the underlying mechanism by which NG-R1 protects against MI/R injury.

DISCUSSION

NG-R1 is a novel phytoestrogen isolated from *P. notoginseng* that is considered to have antioxidative, anti-inflammatory and antiapoptotic properties [39–41]. However, its potential cardioprotective mechanism remains largely unknown. Our current study provides novel insights into the role of NG-R1 in MI/R injury. The new findings include the following: (1) NG-R1 alleviated MI/R-induced infarct size expansion and restored compromised cardiac function; (2) NG-R1 inhibited the activation of TAK1-JNK/p38 signaling and reduced apoptosis; (3) the cardioprotective effects of NG-R1 were nullified by the JNK agonist anisomycin and p38 agonist P79350 in vivo and in vitro; and (4) TAK1 overexpression partially reversed the cardioprotective effect of NG-R1 in vivo and in vitro, but NG-R1 did not provide further protection in TAK1-silenced cardiomyocytes in response to H/R injury. In summary, we provided evidence that NG-R1 protects against MI/R injury by inhibiting JNK/p38 signaling via a TAK1-dependent mechanism.

NG-R1 is an effective monomer of *Panax notoginseng* that exerts a variety of pharmacological effects on the cardiovascular system by protecting endothelial cells, reducing vascular pressure, inhibiting vascular inflammatory reactions and promoting angiogenesis [26, 42–44]. Moreover, NG-R1 can protect cardiomyocytes by inhibiting oxidation and inflammatory and myocardial hypertrophy [28, 30–32]. However, the exact mechanism by which NG-R1 protects against MI/R injury in mice remains largely unknown [45]. It has been reported that NG-R1 protects against H/R injury by upregulating miR-132 levels in H9C2 cells [46]. Consistently, we demonstrated that NG-R1 increased the viability of CMs and ameliorated LDH release in CMs in response to H/R injury. Consistent with previous studies, NG-R1 treatment reduced plasma levels of cTn-I and CK-MB and alleviated the infarct size after MI/R injury in mice [47]. Notably, NG-R1 restored the compromised cardiac function, and improved LVEF and LVFS. Apoptosis is considered to be an important mechanism of cell death in MI/R injury. Due to limited cardiac regeneration, the loss of cardiomyocytes due to apoptosis directly leads to an increase in infarct size, cardiac dysfunction, or even heart failure [48]. The present study confirmed that NG-R1 prevents apoptosis after MI/R injury, as confirmed by the change in TUNEL-positive cells and the protein levels of Bax and Bcl-2 in vivo. Our study also confirmed that NG-R1 directly protects against apoptosis in cardiomyocytes in vitro.

During the pathogenesis of MI/R injury, MAPK signaling plays important roles in apoptosis and inflammation by activating and/or inactivating three critical subfamilies: ERK, JNK, and p38 [12, 34, 48]. ERK signaling mainly mediates cell growth, division and differentiation signals [49]. In cultured neonatal cardiomyocytes, sustained activation of the ERK pathway mediates adaptive cytoprotection [50]. The JNK and p38 cascades, which are specialized transducers of stress and injury responses, mainly transduce inflammatory cytokines, apoptosis and various types of cellular stress signals during MI/R injury [51–53]. Inhibiting the activation of p38 with SB203580 protected against apoptosis in the myocardium [54]. A previous study reported that NG-R1 exerted neuroprotective effects by regulating the PI3K Akt mTOR/JNK pathway in neonatal hypoxic-ischemic injury [30]. NG-R1

inhibited oxidative stress-induced osteoblast dysfunction by modulating the JNK signaling pathway [55]. Consistently, our study demonstrated that p38, JNK and ERK were activated by MI/R and H/R stimulation, but only the activation of JNK and p38 was inhibited by NG-R1. To further determine whether JNK/p38 was indispensable for the protective effect of NG-R1 against MI/R injury, anisomycin (a JNK agonist) and P79350 (a p38 agonist) were used in vivo and in vitro. The results showed that pretreatment with the JNK agonist anisomycin or the p38 agonist P79350 partially abolished the protective effects of NG-R1 in vivo and in vitro. Thus, NG-R1 can protect against MI/R injury by inhibiting the activation of JNK and p38.

TAK1 is an important signaling protein that activates a variety of signaling pathways in response to growth factors, cytokines and microbial products [56, 57]. The activation of the TAK1 is strictly regulated by its binding partners and protein modifications. The activation of TAK1 requires an association with TAK1 binding protein 1, which triggers the phosphorylation of TAK1 in vivo [58, 59]. TAK1 polyubiquitination induces autophosphorylation at Thr187 [60], its activation loop and other sites, including Thr184 and Ser192 [61]. TAK1 plays a critical role in regulating cardiomyocyte death and I/R injury [19, 22, 24]. As a member of the MAPKKK family, activated TAK1 activates the MAPK kinases MKK4 and MKK3/6, which phosphorylate p38 MAPK and JNK, respectively. Therefore, TAK1 activation was examined to determine the exact mechanism by which NG-R1 affects MI/R injury. Previous studies have shown that NG-R1 deactivates the TGFβ1/TAK1 signaling pathway and protects the heart against lung ischemia-reperfusion injury in rabbits [32]. NG-R1 protected WI-38 cells against lipopolysaccharide-induced injury by inhibiting TAK1/JNK signaling pathways [62]. In this study, TAK1 phosphorylation was increased after MI/R injury, and NG-R1 pretreatment inhibited TAK1 phosphorylation in vivo and in vitro. In addition, NG-R1 did not further protect TAK1-silenced cardiomyocytes from H/R injury. Furthermore, our study revealed that H/R-induced TAK1-JNK/p38 signaling activity in CMs was suppressed by NG-R1 treatment, and this effect was almost completely reversed by TAK1 overexpression. Cardiac-specific overexpression of TAK1 abolished the protective effect of NG-R1 on MI/R hearts, which revealed the potential molecular target of NG-R1. NG-R1 exerted cardioprotective effects against I/R injury by inhibiting ER stress in H9C2 and Langendorf-perfused rat hearts [28]. Further analysis showed that NG-R1 inhibited the release of endoplasmic reticulum calcium through PLC and reduced apoptosis in OGD/R rat models [63]. Our previous studies indicated that TAK1 regulated endoplasmic reticulum (ER) stress and apoptosis during MI/R injury [24]. Although we focused on the TAK1 and JNK/p38 pathways in this study, it would be interesting to further confirm the role of ER stress.

This study showed that NG-R1 protects against MI/R injury by inhibiting cardiomyocyte apoptosis and modulating JNK/p38 signaling by deactivating TAK1. The present study revealed the molecular mechanisms of the beneficial effects of NG-R1 and provided a promising therapeutic approach for the treatment of MI/R injury.

AUTHOR CONTRIBUTIONS
JJZ, HQS and XSZ carried out the cell culture, RT-qPCR, Western blotting experiments. JJZ, FFR, QYC and LPW carried out the animal model and echocardiographic analysis. JJZ, HQS, DJW and MPC analyzed the data and wrote the paper. JJZ, JJZ and LL edited the paper. TFL and LL designed the study and supervised the research.

ADDITIONAL INFORMATION

Competing interests: The authors declare no competing interests.

REFERENCES

1. Benjamin EJ, Blaha MJ, Chiuve SE, Cushman M, Das SR, Deo R, et al. Heart Disease and Stroke Statistics-2017 Update: A Report From the American Heart Association. Circulation. 2017;135:e146–146e603.
2. Hausenloy DJ, Yellon DM. Targeting myocardial reperfusion injury–the search continues. N Engl J Med. 2015;373:1073–5.
3. Hausenloy DJ, Yellon DM. Ischaemic conditioning and reperfusion injury. Nat Rev Cardiol. 2016;13:193–209.
4. Heusch G. The coronary circulation as a target of cardioprotection. Circ Res. 2016;118:1643–58.
5. Ruan Y, Zeng J, Jin Q, Chu M, Ji K, Wang Z, et al. Endoplasmic reticulum stress serves an important role in cardiac ischemia/reperfusion injury (Review). Exp Ther Med. 2020;20:268.
6. Sun S, Yu W, Xu H, Li C, Zou R, Wu NN, et al. TBC1D15-Drp1 interaction-mediated mitochondrial homeostasis confers cardioprotection against myocardial ischemia/reperfusion injury. Metabolism. 2022;134:155239.
7. Chang X, Lochner A, Wang HH, Wang S, Zhu H, Ren J, et al. Coronary microvascular injury in myocardial infarction: perception and knowledge for mitochondrial quality control. Theranostics. 2021;11:6766–85.
8. Paskeh M, Asadi A, Mirzaei S, Hashemi M, Entezari M, Raesi R, et al. Targeting AMPK signaling in ischemic/reperfusion injury: from molecular mechanism to pharmacological interventions. Cell Signal. 2022;94:110323.
9. Ferdinandy P, Schulz R, Baxter GF. Interaction of cardiovascular risk factors with myocardial ischemia/reperfusion injury, preconditioning, and postconditioning. Pharmacol Rev. 2007;59:418–58.
10. Fan Q, Tao R, Zhang H, Xie H, Lu L, Wang T, et al. Dectin-1 contributes to myocardial ischemia/reperfusion injury by regulating macrophage polarization and neutrophil infiltration. Circulation. 2019;139:663–78.
11. Yi Q, Tan FH, Tan JA, Chen XH, Xiao Q, Liu YH, et al. Minocycline protects against myocardial ischemia/reperfusion injury in rats by upregulating MCPIP1 to inhibit NF-κB activation. Acta Pharmacol Sin. 2019;40:1019–28.
12. Steenbergen C. The role of p38 mitogen-activated protein kinase in myocardial ischemia/reperfusion injury; relationship to ischemic preconditioning. Basic Res Cardiol. 2002;97:276–85.
13. Chen X, Li X, Zhang W, He J, Xu B, Lei B, et al. Activation of AMPK inhibits inflammatory response during hypoxia and reoxygenation through modulating JNK-mediated NF-κB pathway. Metabolism 2018;83:256–70.
14. Ottani A, Galantucci M, Ardimento E, Neri L, Canalini F, Calevro A, et al. Modulation of the JAK/ERK/STAT signaling in melanocortin-induced inhibition of local and systemic responses to myocardial ischemia/reperfusion. Pharmacol Res. 2013;72:1–8.
15. Feng M, Wang L, Chang S, Yuan P. Penehyclidine hydrochloride regulates mitochondrial dynamics and apoptosis through p38MAPK and JNK signal pathways and provides cardioprotection in rats with myocardial ischemia-reperfusion injury. Eur J Pharm Sci. 2018;121:243–50.
16. Forouzanfar MH, Moran AE, Flaxman AD, Roth G, Mensah GA, Ezzati M, et al. Assessing the global burden of ischemic heart disease, part 2: analytic methods and estimates of the global epidemiology of ischemic heart disease in 2010. Glob Heart. 2012;7:331–42.
17. Benjamin EJ, Virani SS, Callaway CW, Chamberlain AM, Chang AR, Cheng S, et al. Heart Disease and Stroke Statistics-2018 Update: A Report From the American Heart Association. Circulation. 2018;137:e67–67e492.
18. Lakota J. Molecular mechanism of ischemia - Reperfusion injury after myocardial infarction and its possible targeted treatment. Int J Cardiol. 2016;220:571–2.
19. Li L, Chen Y, Doan J, Murray J, Molkentin JD, Liu Q. Transforming growth factor β-activated kinase 1 signaling pathway critically regulates myocardial survival and remodeling. Circulation. 2014;130:2162–72.
20. Wei Q, Tu Y, Zuo L, Zhao J, Chang Z, Zou Y, et al. MiR-345-3p attenuates apoptosis and inflammation caused by oxidized low-density lipoprotein by targeting TRAF6 via TAK1/p38/NF-κB signaling in endothelial cells. Life Sci. 2020;241:117142.
21. Wang J, Ma J, Nie H, Zhang XJ, Zhang P, She ZG, et al. Hepatic regulator of G protein signaling 5 ameliorates nonalcoholic fatty liver disease by suppressing transforming growth factor beta-activated kinase 1-c-Jun-N-terminal kinase/p38 signaling. Hepatology. 2021;73:104–25.
22. Wang X, Mao W, Fang C, Tian S, Zhu X, Yang L, et al. Dusp14 protects against hepatic ischaemia-reperfusion injury via Tak1 suppression. J Hepatol. 2017;S0168-8278:32275–4.
23. Song H, Wang P, Liu J, Wang C. Panax notoginseng preparations for unstable angina pectoris: a systematic review and Meta-analysis. Phytother Res. 2017;31:1162–72.
24. Zeng J, Jin Q, Ruan Y, Sun C, Xu G, Chu M, et al. Inhibition of TGFβ-activated protein kinase 1 ameliorates myocardial ischaemia/reperfusion injury via endoplasmic reticulum stress suppression. J Cell Mol Med. 2020;24:6846–59.
25. Chan P, Thomas GN, Tomlinson B. Protective effects of trilinolein extracted from panax notoginseng against cardiovascular disease. Acta Pharmacol Sin. 2002;23:1157–62.
26. Liu J, Wang Y, Qiu L, Yu Y, Wang C. Saponins of Panax notoginseng: chemistry, cellular targets and therapeutic opportunities in cardiovascular diseases. Expert Opin Investig Drugs. 2014;23:523–39.
27. Liu H, Yang J, Yang W, Hu S, Wu Y, Zhao B, et al. Focus on notoginsenoside R1 in metabolism and prevention against human diseases. Drug Des Devel Ther. 2020;14:551–65.
28. Yu Y, Sun G, Luo Y, Wang M, Chen R, Zhang J, et al. Cardioprotective effects of Notoginsenoside R1 against ischemia/reperfusion injuries by regulating oxidative stress- and endoplasmic reticulum stress- related signaling pathways. Sci Rep. 2016;6:21730.
29. Sun B, Xiao J, Sun XB, Wu Y. Notoginsenoside R1 attenuates cardiac dysfunction in endotoxemic mice: an insight into oestrogen receptor activation and PI3K/Akt signalling. Br J Pharmacol. 2013;168:1758–70.
30. Tu L, Wang Y, Chen D, Xiang P, Shen J, Li Y, et al. Protective effects of notoginsenoside R1 via regulation of the PI3K-Akt-mTOR/JNK pathway in neonatal cerebral hypoxic-ischemic brain injury. Neurochem Res. 2018;43:1210–26.
31. Liu WJ, Tang HT, Jia YT, Ma B, Fu JF, Wang Y, et al. Notoginsenoside R1 attenuates renal ischemia-reperfusion injury in rats. Shock. 2010;34:314–20.
32. Ge ZR, Xu MC, Huang YU, Zhang CJ, Lin JE, Ruan CW. Cardioprotective effect of notoginsenoside R1 in a rabbit lung remote ischemic postconditioning model via activation of the TGF-β1/TAK1 signaling pathway. Exp Ther Med. 2016;11:2341–8.
33. Zhu T, Wang L, Tian F, Zhao X, Pu XP, Sun GB, et al. Anti-ischemia/reperfusion injury effects of notoginsenoside R1 on small molecule metabolism in rat brain after ischemic stroke as visualized by MALDI-MS imaging. Biomed Pharmacother. 2020;129:110470.
34. An S, Wang X, Shi H, Zhang X, Meng H, Li W, et al. Apelin protects against ischemia-reperfusion injury in diabetic myocardium via inhibiting apoptosis and oxidative stress through PI3K and p38-MAPK signaling pathways. Aging. 2020;12:25120–37.
35. Guo X, Yin H, Li L, Chen Y, Li J, Doan J, et al. Cardioprotective role of tumor necrosis factor receptor-associated factor 2 by suppressing apoptosis and necroptosis. Circulation. 2017;136:729–42.
36. Guo X, Yin H, Chen Y, Li L, Li J, Liu Q. TAK1 regulates caspase 8 activation and necroptotic signaling via multiple cell death checkpoints. Cell Death Dis. 2016;7:e2381.
37. Zhang XJ, Liu X, Hu M, Zhao GJ, Sun D, Cheng X, et al. Pharmacological inhibition of arachidonate 12-lipoxygenase ameliorates myocardial ischemia-reperfusion injury in multiple species. Cell Metab. 2021;33:2059–75.e10.
38. Wang Q, Feng J, Wang J, Zhang X, Zhang D, Zhu T, et al. Disruption of TAB1/p38α interaction using a cell-permeable peptide limits myocardial ischemia/reperfusion injury. Mol Ther. 2013;21:1668–77.
39. Zheng QN, Wei XH, Pan CS, Li Q, Liu YY, Fan JY, et al. QiShenYiQi Pills(®) ameliorates ischemia/reperfusion-induced myocardial fibrosis involving RP S19-mediated TGFβ1/Smads signaling pathway. Pharmacol Res. 2019;146:104272.
40. Xiao J, Zhu T, Yin YZ, Sun B. Notoginsenoside R1, a unique constituent of *Panax notoginseng*, blinds proinflammatory monocytes to protect against cardiac hypertrophy in ApoE$^{(-/-)}$ mice. Eur J Pharmacol. 2018;833:441–50.
41. Zhang B, Zhang J, Zhang C, Zhang X, Ye J, Kuang S, et al. Notoginsenoside R1 protects against diabetic cardiomyopathy through activating estrogen receptor α and its downstream signaling. Front Pharmacol. 2018;9:1227.
42. Zhou P, Xie W, He S, Sun Y, Meng X, Sun G, et al. Ginsenoside Rb1 as an anti-diabetic agent and its underlying mechanism analysis. Cells. 2019;8:204.
43. Liu H, Lu X, Hu Y, Fan X. Chemical constituents of *Panax ginseng* and *Panax notoginseng* explain why they differ in therapeutic efficacy. Pharmacol Res. 2020;161:105263.
44. Han JY, Li Q, Ma ZZ, Fan JY. Effects and mechanisms of compound Chinese medicine and major ingredients on microcirculatory dysfunction and organ injury induced by ischemia/reperfusion. Pharmacol Ther. 2017;177:146–73.
45. Duan L, Xiong X, Hu J, Liu Y, Li J, Wang J. *Panax notoginseng* saponins for treating coronary artery disease: a functional and mechanistic overview. Front Pharmacol. 2017;8:702.
46. Jin Z, Gan C, Luo G, Hu G, Yang X, Qian Z, et al. Notoginsenoside R1 protects hypoxia-reoxygenation deprivation-induced injury by upregulation of miR-132 in H9c2 cells. Hum Exp Toxicol. 2021;40:S29–29S38.
47. Xia KP, Ca HM, Shao CZ. Protective effect of notoginsenoside R1 in a rat model of myocardial ischemia reperfusion injury by regulation of Vitamin D3 upregulated protein 1/NF-κB pathway. Pharmazie. 2015;70:740–4.

Notoginsenoside R1 protects against myocardial ischemia/reperfusion injury
JJ Zeng et al.

1379

48. Freude B, Masters TN, Robicsek F, Fokin A, Kostin S, Zimmermann R, et al. Apoptosis is initiated by myocardial ischemia and executed during reperfusion. J Mol Cell Cardiol. 2000;32:197–208.

49. Bassat E, Mutlak YE, Genzelinakh A, Shadrin IY, Baruch Umansky K, Yifa O, et al. The extracellular matrix protein agrin promotes heart regeneration in mice. Nature. 2017;547:179–84.

50. Yue TL, Wang C, Gu JL, Ma XL, Kumar S, Lee JC, et al. Inhibition of extracellular signal-regulated kinase enhances ischemia/reoxygenation-induced apoptosis in cultured cardiac myocytes and exaggerates reperfusion injury in isolated perfused heart. Circ Res. 2000;86:692–9.

51. Xu W, Zhang L, Zhang Y, Zhang K, Wu Y, Jin D. TRAF1 exacerbates myocardial ischemia reperfusion Injury via ASK1-JNK/p38 signaling. J Am Heart Assoc. 2019;8:e012575.

52. Engelbrecht AM, Niesler C, Page C, Lochner A. p38 and JNK have distinct regulatory functions on the development of apoptosis during simulated ischaemia and reperfusion in neonatal cardiomyocytes. Basic Res Cardiol. 2004;99:338–50.

53. Shvedova M, Anfinogenova Y, Atochina-Vasserman EN, Schepetkin IA, Atochin DN. c-Jun N-Terminal Kinases (JNKs) in myocardial and cerebral ischemia/reperfusion injury. Front Pharmacol. 2018;9:715.

54. Barancik M, Htun P, Strohm C, Kilian S, Schaper W. Inhibition of the cardiac p38-MAPK pathway by SB203580 delays ischemic cell death. J Cardiovasc Pharmacol. 2000;35:474–83.

55. Li X, Lin H, Zhang X, Jaspers RT, Yu Q, Ji Y, et al. Notoginsenoside R1 attenuates oxidative stress-induced osteoblast dysfunction through JNK signalling pathway. J Cell Mol Med. 2021;25:11278–89.

56. Ge B, Gram H, Di Padova F, Huang B, New L, Ulevitch RJ, et al. MAPKK-independent activation of p38alpha mediated by TAB1-dependent autophosphorylation of p38alpha. Science. 2002;295:1291–4.

57. Li J, Miller EJ, Ninomiya-Tsuji J, Russell RR 3rd, Young LH. AMP-activated protein kinase activates p38 mitogen-activated protein kinase by increasing recruitment of p38 MAPK to TAB1 in the ischemic heart. Circ Res. 2005;97:872–9.

58. Shibuya H, Yamaguchi K, Shirakabe K, Tonegawa A, Gotoh Y, Ueno N, et al. TAB1: an activator of the TAK1 MAPKKK in TGF-beta signal transduction. Science. 1996;272:1179–82.

59. Sakurai H, Miyoshi H, Mizukami J, Sugita T. Phosphorylation-dependent activation of TAK1 mitogen-activated protein kinase kinase kinase by TAB1. FEBS Lett. 2000;474:141–5.

60. Yu Y, Ge N, Xie M, Sun W, Burlingame S, Pass AK, et al. Phosphorylation of Thr-178 and Thr-184 in the TAK1 T-loop is required for interleukin (IL)−1-mediated optimal NFkappaB and AP-1 activation as well as IL-6 gene expression. J Biol Chem. 2008;283:24497–505.

61. Hashimoto K, Simmons AN, Kajino-Sakamoto R, Tsuji Y, Ninomiya-Tsuji J. TAK1 regulates the Nrf2 antioxidant system through modulating p62/SQSTM1. Antioxid Redox Signal. 2016;25:953–64.

62. Qian D, Shao X, Li Y, Sun X. Notoginsenoside R1 protects WI-38 cells against lipopolysaccharide-triggered injury via adjusting the miR-181a/TLR4 axis. J Cell Biochem. 2019;120:19764–74.

63. Wang Y, Tu L, Li Y, Chen D, Liu Z, Hu X, et al. Notoginsenoside R1 alleviates oxygen-glucose deprivation/reoxygenation injury by suppressing endoplasmic reticulum calcium release via PLC. Sci Rep. 2017;7:16226.